1

Imaging Magnetic Microspectroscopy

W. Kuch

There are several well established techniques for spectroscopy of magnetic films and surfaces that are commonly employed when information about electronic states, binding properties, or element-resolved magnetic properties is required. The reduction in lateral size that goes along with the soaring extent to which magnetic elements and devices are used or planned to be used in technological applications in magnetic sensors, data storage, or magneto-electronics demands magnetic spectroscopic information on a microscopic lateral length scale. Thus, the combination of magnetic spectroscopy and microscopy into what is commonly termed microspectroscopy or spectromicroscopy would be ideal for the study of small magnetic structures.

This chapter explains the combination of photoelectron emission microscopy (PEEM) and X-ray magnetic circular dichroism (XMCD) in absorption for imaging XMCD-PEEM microspectroscopy. In a PEEM, an electrostatic electron optics creates a magnified image of the secondary electron intensity distribution at the sample surface. When excited by soft X-rays, the image intensity can thus be regarded as a local electron yield probe of X-ray absorption. In XMCD, the measurement of the total electron yield of the sample is frequently used to determine the X-ray absorption as a function of photon energy and helicity of the circularly polarized radiation. Consequently, scanning the photon energy and recording PEEM images at each photon energy step for both helicities results in a microspectroscopic data set that allows one to extract the full information that is usually obtained from XMCD spectra for each single pixel of the images. Of particular interest is therefore the application of the so-called sum rules to extract the effective spin moment and the orbital moment, projected onto the direction of incoming light. This chapter starts with a short overview of magnetic microspectroscopy techniques in comparison to XMCD-PEEM microspectroscopy. The basics of the underlying spectroscopic and microscopic methods are briefly explained in Sect. 1.2. Important experimental aspects inherent to XMCD-PEEM microspectroscopy are discussed in Sect. 1.3. Finally, in Sect. 1.4, two recent examples of application of XMCD-PEEM microspectroscopy are presented, in which the method has proven beneficial for the study of interesting issues in the field of ultrathin magnetic films.

1.1 Microspectroscopy and Spectromicroscopy – An Overview

The terms "microspectroscopy" and "spectromicroscopy" both refer to techniques that combine spectroscopy and microscopy. "Spectromicroscopy" is commonly used to describe microscopic imaging techniques in which the image contrast is due to spectroscopic details. The acquired images are then related to a certain energy of either electrons or photons. "Microspectroscopy," on the other hand, is primarily used to describe techniques in which spectroscopic information is obtained from a small area on a sample. In terms of the dependence of information gained, spectromicroscopy is thus a technique that yields data as a function of the two space coordinates for a certain value of the energy coordinate, whereas microspectroscopy delivers data as a function of energy for a fixed pair of values of the space coordinates. The consequent extension of both spectromicroscopy and microspectroscopy would be to get the full spectroscopic *and* spatial information in the same measurement. That is, data are obtained as a function of all three variables, namely, the two space coordinates and energy. In that limit, "spectromicroscopy" and "microspectroscopy" become identical. The topic of this contribution is the combination of X-ray magnetic circular dichroism (XMCD) and photoelectron emission microscopy (PEEM) for the measurement of such a three-dimensional data set. It may be considered as either full-image microspectroscopy or full-energy spectromicroscopy, where we (arbitrarily) have chosen the former name, and thus will refer to it as "microspectroscopy". In all cases, the extension to full-image microspectroscopy, or imaging microspectroscopy, represents a considerably higher experimental effort, and it will be only practical if the gain in information makes it worthwhile.

In this section, a short overview of some microspectroscopic and spectromicroscopic techniques used for the investigation of magnetic samples is given, and the use of XMCD-PEEM as an ideal imaging microspectroscopic technique is motivated. A more comprehensive overview of spectromicroscopic techniques for non-magnetic applications can be found in [1].

1.1.1 Scanning Techniques

In microscopy, one can generally distinguish between scanning techniques and techniques that use parallel imaging. We will start with the scanning techniques. A scanning technique that is commonly employed at most synchrotron light sources and can be used for magnetic microspectroscopy is scanning X-ray microscopy (SXM). The incident X-ray radiation from the synchrotron is focused with appropriate X-ray optics, for example, by Fresnel zone plates, into a small spot on the sample. Depending on the photon energy range, spot sizes smaller than 200 nm have been achieved [2, 3]. In plain microscopy applications, the sample is scanned and the transmitted X-rays generate the microscopic image. With only minor modifications such setups can easily be used for spectromicroscopy or microspectroscopy. For magnetic microspectroscopy in the simplest case, the dependence of the transmitted, absorbed, or reflected X-ray intensity on photon energy is recorded. Magnetic contrast is obtained from the dependence on magnetization direction of the X-ray

absorption cross section at elemental absorption edges when circular polarization is used (see Sect. 1.2.1). Another variant includes electron spectroscopy, where emitted electrons of a certain kinetic energy are detected [4]. Here, magnetic contrast can be obtained from magnetic dichroism in photoelectron spectroscopy, which is the difference in photoelectron intensity upon variation of magnetization direction or X-ray polarization [5]. Since the magnetic contrast is higher in absorption, only this has been used for magnetic imaging [6,7]. The advantage of scanning X-ray microscopy is that the microscopy component of the technique is completely in the excitation path, so that on the detection path standard spectrometers can be used to provide the spectroscopy component. The energy resolution for electron detection can thus be chosen to be the same as in plain photoelectron or Auger electron spectroscopy. For imaging microspectroscopy, however, the disadvantage, as in all scanning techniques, is that the time needed for a complete scan of both the sample position and the energy can be quite long.

Another scanning spectromicroscopic technique for imaging magnetic properties is spin-polarized scanning tunneling microscopy, in which the spin-dependence in electron tunneling between ferromagnets is used as a contrast mechanism (see Chaps. 9,10). In one approach, the tip magnetization is periodically reversed (Chap. 9), while another approach relies on differential electron tunneling spectroscopy (Chap. 10). In the latter, the bias voltage between a magnetic tip and the sample is set to an energy at which the dependence of the tunnel current on the direction of sample magnetization is maximized [8,9]. Without changing the experimental setup microspectroscopy can also be performed. For this, the tip position is kept fixed and the bias voltage is varied. In principle imaging scanning tunneling microspectroscopy is also possible. Due to restrictions in acquisition times, however, in most cases this is used only to find the best energy for obtaining magnetic domain images.

For the imaging of magnetic domains, laser scanning Kerr microscopy has also been used [10]. The magneto-optical Kerr effect using visible light is a commonly employed method to measure magnetization curves. The spectroscopic variant, Kerr spectroscopy, where the wavelength of the exciting laser light is scanned, is used for the characterization of electronic properties [11]. No reports exist, however, of imaging scanning Kerr microspectroscopy measurements.

As mentioned before, in general, the disadvantage of all scanning techniques for imaging microspectroscopy is that three parameters, namely, two space coordinates *and* the energy, need to be scanned step by step, which can make it a rather lengthy undertaking. Consequently, in most cases, the relation between effort and benefit does not favor imaging scanning microspectroscopy.

1.1.2 Imaging Techniques

Parallel imaging techniques have the advantage over scanning techniques in that for imaging microspectroscopy only the energy needs to be scanned, while at each energy step a complete image is acquired. Parallel imaging techniques may, therefore, be accelerated to achieve feasible measuring times even for full image microspectroscopy. The individual images are equivalent to two-dimensional sets of data points, which

are acquired in parallel. Parallel imaging of magnetic spectroscopic information is based either on magneto-optical effects or on magneto-dichroic effects in electron spectroscopy after optical excitation.

An example of magneto-optical effects [12] is the magneto-optical Kerr effect using visible light, as already mentioned in the previous section. In the microscopic variant, optical microscopy is used to convert the magneto-optical information into a domain image of the sample [10]. The gain in information that would result from the combination of Kerr microscopy with wavelength scanning Kerr spectroscopy, however, does not seem worth the effort, since no imaging Kerr microspectroscopy has been reported in literature up until now.

This differs in the range of soft X-rays, where elemental core level absorption edges are accessed. The optical constants vary strongly in the vicinity of these edges and depend on the magnetization of the sample. The absorption of circularly polarized X-rays at the absorption edges depends on the relative orientation between light helicity and magnetization direction. This mechanism, which will be presented in the following section, is named X-ray magnetic circular dichroism (XMCD) in absorption, and is the first choice for obtaining magnetic contrast in imaging. It has been demonstrated, though, that in principle magnetic circular dichroism in angle-resolved photoemission can also be used to obtain magnetic contrast in photoelectron spectromicroscopy. Images obtained in an imaging hemispherical electron analyzer from Fe $3p$ photoelectrons after off-resonant excitation with circular polarization exhibited a weak magnetic contrast [13]. In a more recent paper, magnetic contrast was claimed even using unpolarized light from an X-ray tube and magnetic dichroism in Fe $2p$ photoemission [14]. The signal-to noise ratio, however, is significantly worse in the photoemission case compared to images obtained in the same instrument using XMCD in absorption to generate magnetic contrast [15, 16].

Two ways can generally be used to image the local X-ray absorption: either by imaging photons, or by imaging emitted electrons. Imaging the transmitted photons has been successfully performed for magnetic spectromicroscopic domain imaging in a transmission X-ray microscope [17]. The sample is thereby prepared such that its total thickness allows the transmission of soft X-rays, and a zone plate–based X-ray optics is used to create the image of the transmitted beam. In general, the drawback for microspectroscopy with photon imaging techniques stems from problems due to the energy dependence of the focal length of X-ray optics, in particular, of zone plates. The magnification and focusing of the resulting image, therefore, varies during a photon energy scan, which leads to a significant blurring of the image if no correction, for example, by a sophisticated image processing software, is performed.

In that respect, the imaging of the distribution of emitted electron intensity for microspectroscopic purposes is clearly easier. Since just the X-ray absorption needs to be detected as a function of photon energy, no explicit energy filtering of the electrons is necessary and the high intensity secondary electrons may be used. X-ray optics, if any, are used only for the illumination of the imaged area of the sample. Different types of electron optics have been employed successfully for XMCD-based spectromicroscopic imaging of magnetic domains, all of which are classified under the name "electron emission microscopy". While in most of the more recent work fully

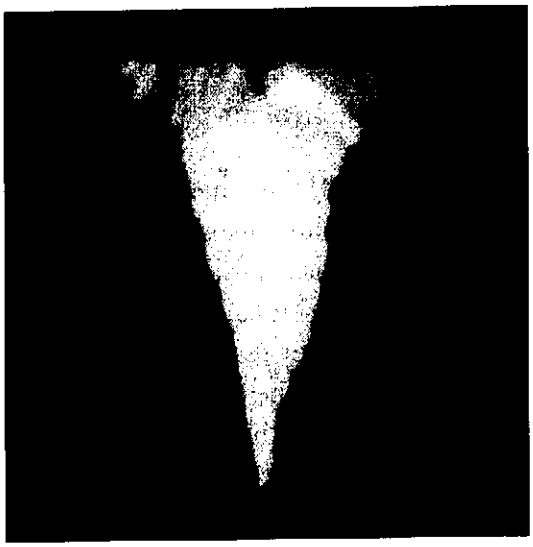

Fig. 1.1. Magnetic domain image of a triangular microstructure of 30-nm-thick polycrystalline Co on Si using a PEEM and XMCD. Field of view is $40 \times 40\mu m^2$

electrostatic photoelectron emission microscopes (PEEMs) (see Sect. 1.2.2) were used [18–23], an imaging hemispherical electron analyzer [15,16], and in [24] a low energy electron microscope (LEEM, [25,26]) have also been employed. Note that the latter is different from magnetic imaging by spin-polarized LEEM, which is presented in Chap. 6. Figure 1.1 shows an example of a domain image taken with a PEEM. It shows a lithographic triangular microstructure of 30-nm-thick polycrystalline Co. Different grayscale contrast represents different directions of magnetization, where bright means pointing up, dark pointing down, and intermediate gray indicates a horizontal magnetization direction [27].

The advantage of extending XMCD-based spectromicroscopy with electron detection to imaging microspectroscopy is obvious: Experimentally, it is quite straightforward if some aspects, as outlined in Sect. 1.3, are considered. XMCD is a widely used and comparably well understood spectroscopic technique, so there is a significant gain in quantitative information from full-image microspectroscopy compared with the acquisition of spectromicroscopic images; this will be discussed in Sect. 1.2.1. Finally, due to the availability of high-brilliance insertion-device beamlines at third-generation synchrotron radiation light sources, the time required for recording three-dimensional data sets for imaging microspectroscopy is approaching feasibility while still maintaining reasonable spatial resolution. This will be demonstrated by selected examples in Sect. 1.4.

A further advantage of X-ray absorption–based spectromicroscopy is that by using linearly polarized X-rays, a magnetic-dichroic signal can also be obtained from oxidic antiferromagnets [28,29]. The use of this X-ray linear magnetic dichroism for the imaging of antiferromagnetic domains is outlined in Chap. 2.

In the remainder of this chapter, PEEM is assumed as the electron emission microscopy technique for magnetic X-ray absorption spectroscopy. This is due to the existing work in this field, although, most of what is described is also valid for any other type of electron emission microscopy.

1.2 Basics

1.2.1 X-Ray Magnetic Circular Dichroism

Since its experimental discovery [30], magnetic circular dichroism in soft X-ray absorption has developed into a widely used technique for the element-specific characterization of magnetic films and multilayers. This is in part due to the so-called sum rules that have been proposed to deduce quantitative magnetic information from XMCD spectra [31, 32]. Other reasons for the widespread use of XMCD are: The magnetism-related changes in the absorption cross section are quite large; there are several synchrotron radiation light sources around the world providing X-rays of tunable wavelength, and it is comparatively easy to measure X-ray absorption from the total photoelectron yield, where only the sample current has to be detected.

This section is aimed at providing the reader who is not familiar with XMCD spectroscopy with the basic ideas in order to follow the remainder of the chapter. More comprehensive introductions can be found elsewhere [12, 22, 33–36].

We will restrict ourselves to the $L_{2,3}$ absorption edges of $3d$ transition metals, i.e., the onset of excitation of transitions of $2p$ core electrons to empty states above the Fermi level. Let us for the moment consider absorption in a paramagnet. An explanation of X-ray absorption spectroscopy in a one-electron description is shown in Fig. 1.2. The left upper panel shows a schematic representation of the occupied density of states of the $2p$ core levels. The important point here is that because of spin-orbit interaction, the $2p$ states are energetically split into the clearly separated $2p_{1/2}$ and $2p_{3/2}$ levels. Any further splitting into sublevels is not important here. Absorption of X-rays by the excitation of electronic transitions from the $2p$ states is determined by the occupied density of states of the $2p$ core electrons and the unoccupied density of states available for these transitions above the Fermi energy (E_F). The latter is schematically shown in the upper right panel, where the shaded area represents the unoccupied states. The contribution from states of predominantly s, p character is represented by flat energy dependence, whereas d states are shown as sharp peaks around E_F. The resulting absorption spectrum is obtained from the convolution of the occupied density of states of the left upper panel and the unoccupied density of states of the right upper panel. Finite experimental photon energy resolution has to be taken into account by an additional convolution with a Gaussian. A typical $L_{2,3}$ absorption spectrum is shown in the bottom panel of Fig. 1.2. It is seen that the absorption signal related to transitions into empty $3d$ states shows up as two peaks at the energetic positions of the $2p_{1/2}$ and $2p_{3/2}$ states, whereas transitions into unoccupied s, p states give rise to a step-like background. Since the magnetic moment of the $3d$ transition metals is mainly governed by $3d$ valence electrons, the latter is usually subtracted as a step function with relative step heights of 2:1 [37], according to the occupation of the $2p_{3/2}$ and $2p_{1/2}$ core states, as shown in the bottom panel of Fig. 1.2.

If $2p \rightarrow 3d$ transitions are excited by circularly polarized radiation, these transitions exhibit a spin polarization because of selection rules [38]. In other words,

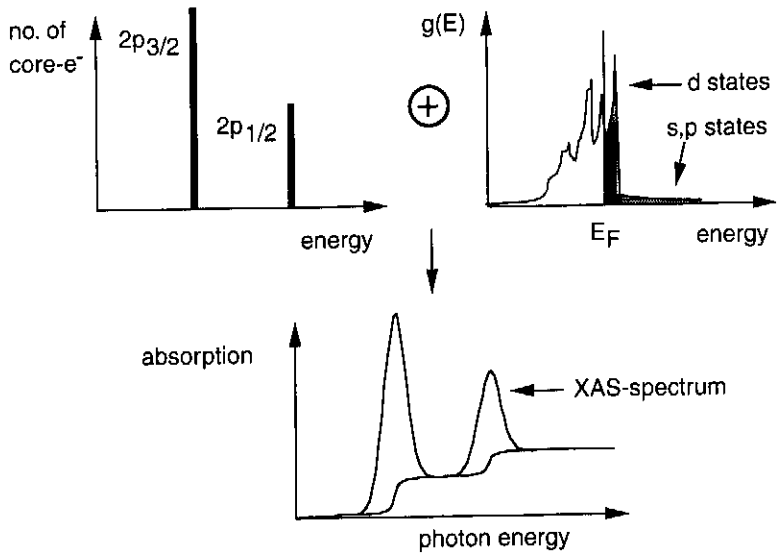

Fig. 1.2. Schematic explanation of X-ray absorption spectroscopy (XAS). The absorption spectrum shown in the bottom panel results from the convolution of the occupied density of states of the core levels (*upper left*) and the unoccupied density of states $g(E)$ of the valence states (*upper right, shaded area*). The contribution from s, p states is usually approximated and subtracted in the form of a step function (*bottom panel*)

for a certain light helicity, more electrons of one spin direction with respect to the direction of the incoming light are excited into the unoccupied $3d$ states than of the other spin direction. In a paramagnet, this does not lead to a change in absorption intensity, since the number of unoccupied states is equal for both spin directions. In a ferromagnet, however, the density of unoccupied states is different for electrons of spin parallel or antiparallel to the magnetization direction, leading to a spin magnetic moment defined by the difference in occupation. This is explained in Fig. 1.3. It shows a schematic representation of the spin resolved density of states, separated into density of states of majority spin electrons at the top and density of states of minority spin electrons at the bottom. If magnetization and light incidence are aligned with each other to some degree, there are consequently more possible transitions for one direction of light helicity than for the other. This leads to a difference in absorption for opposite light helicity. In a dichroism spectrum, calculated as the difference between absorption spectra for opposite helicity, a non-zero difference will show up at the energy positions of the peaks related to transitions from the $2p_{3/2}$ and $2p_{1/2}$ levels into the empty $3d$-like states. Since the spin polarization of $2p_{3/2} \rightarrow 3d$ transitions has an opposite sign than that of the spin polarization of $2p_{1/2} \rightarrow 3d$ transitions [12,35], the dichroism at the L_3 and L_2 edge will have an opposite sign, i.e., the difference curve will show peaks of opposite sign at the energy positions of the L_3 and the L_2 edge. This is shown schematically for the (hypothetical) case of a material with only a spin moment μ_S in the top panel of Fig. 1.4. There, the difference curve between absorption spectra taken with opposite helicity of the circularly polarized light is depicted, which exhibits a positive peak at the L_3 edge, a negative peak at the L_2 edge, and zero elsewhere. The spin polarization of $2p_{1/2} \rightarrow 3d$ transitions is twice

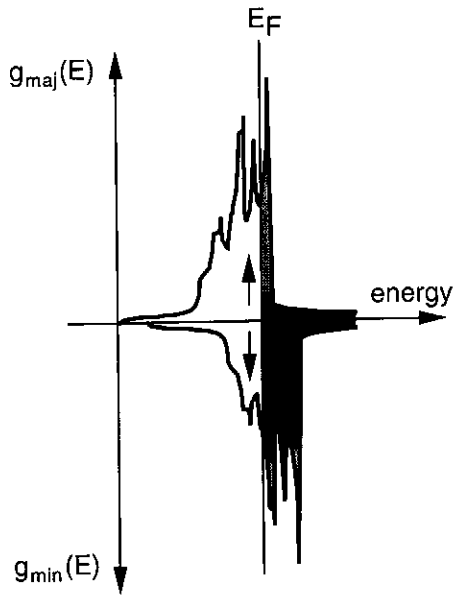

Fig. 1.3. Schematic representation of density of states of a ferromagnetic metal. Shown is the spin resolved density of states for majority electrons $g_{\mathrm{maj}}(E)$ in the positive y direction, and the spin resolved density of states for minority electrons $g_{\mathrm{min}}(E)$ in the negative y direction. The shaded areas are unoccupied density of states above the Fermi energy E_{F} available for $2p \rightarrow 3d$ transitions

as large as the spin polarization of $2p_{3/2} \rightarrow 3d$ transitions. On the other hand, the absorption at the L_3 edge is twice as high as at the L_2 edge because of core hole occupation (cf. Fig. 1.2). Together both lead to an equal size of the dichroism at the two edges, as schematically plotted in the topmost panel of Fig. 1.4.

$2p \rightarrow 3d$ transitions excited by circularly polarized radiation are not only spin polarized, but also show an orbital "polarization." This is a direct consequence of the absorption of a circularly polarized photon with angular momentum $\Delta m = \pm 1$ [12,35]. Both the $2p_{1/2} \rightarrow 3d$ and $2p_{3/2} \rightarrow 3d$ transitions show the same sign and same magnitude of orbital polarization. If a sample possesses a non-zero orbital magnetic moment, this means that the unoccupied states (and also the occupied states) have a non-zero net angular momentum. Let us consider the (hypothetical) case of a metal with only an orbital moment and no spin moment. In this case, there will again be a non-zero dichroism at the L_3 and L_2 edges, but this time with an equal sign at the two edges. Because of the different number of $2p_{1/2}$ and $2p_{3/2}$ electrons, the resulting dichroism at the L_3 edge is twice as large as at the L_2 edge (middle panel of Fig. 1.4).

A real sample will have both spin and orbital magnetic moments. The two extreme cases shown in the top and center panels of Fig. 1.4 define an orthonormal basis for the measured XMCD spectrum from a real sample (bottom panel of Fig. 1.4), which will be a superposition of both. The experimental spectrum can thus be decomposed unambiguously into its spin and orbital basis functions. This is what is done by the so-called sum rules [31,32].

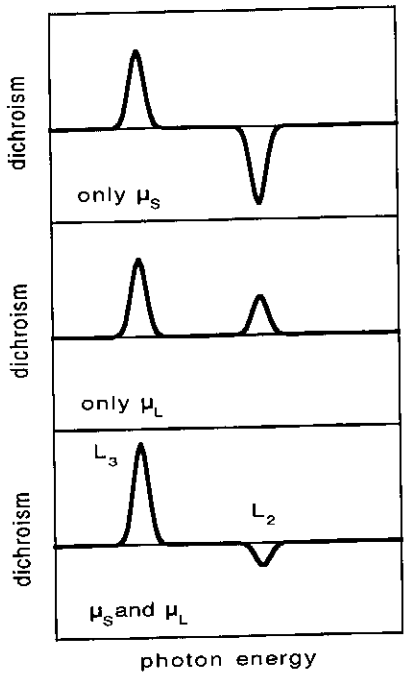

Fig. 1.4. Schematic explanation of sum rule analysis of XMCD spectra to obtain spin and orbital moments. Shown is the decomposition of an XMCD spectrum (*bottom*) into its components resulting from spin moment μ_S (*top*) and orbital moment μ_L (*center*)

It has to be mentioned that what is extracted as the "spin moment" from the sum rules is an effective spin moment $\mu_{S,eff}$ [32], which includes the actual spin magnetic moment μ_S plus a contribution from the magnetic dipole term. The latter is zero in the bulk of cubic crystals, but can be of the same order as the orbital moment in ultrathin films [39].

Although the derivation of the sum rules was done under simplifying assumptions, and there has been some dispute about their applicability [34,37,40–43], they seem to yield reasonable results for the 3*d* transition metals [34,37,44–46]. Together with the element-selectivity of X-ray absorption spectroscopy at core level absorption edges they provide a quite powerful tool for the quantitative investigation of magnetic materials.

1.2.2 Photoelectron Emission Microscopy

Photoelectron emission microscopy (PEEM) belongs to the parallel imaging electron microscopies. The name "photoelectron" is due to its use in metallurgy in early years, when threshold excitation of photoelectrons at the vacuum level by illumination with Hg discharge lamps was used for the acquisition of work function contrast images [47]. For excitation with higher photon energies, which will be considered in this chapter, low energy secondary electrons are dominant in the imaging process. We nevertheless stick to the name PEEM, although in that case "secondary electron emission microscope" would be more correct.

After the introduction of ultrahigh-vacuum compatible instruments [48, 49], PEEM has been used for the study of surfaces and surface reactions [50–53]. Incorporating a magnetic electron beam splitter allowed the excitation by low energy electrons (LEEM, low energy electron microscopy [25, 54]), which yields additional information about the surface structure and morphology. LEEM can also be employed for magnetic imaging if spin-polarized electrons are used; this is described in Chap. 6. The availability of synchrotron light sources for excitation with X-rays of tunable energy opened a new field of application for PEEMs [55], in which resonant X-ray absorption at elemental core levels is used to image the distribution of different elements at the sample surface.

In a PEEM, in contrast to transmission electron microscopy, the electrons that are used for the imaging do not have a well-defined energy and momentum. To get a sharp image it is therefore necessary to limit the range of electron energies and emission angles. In a PEEM, this is achieved by passing the accelerated electrons through a pinhole aperture, the so-called contrast aperture. A higher lateral resolution is thereby achieved at the expense of intensity, and vice versa.

Figure 1.5 shows the schematic setup of an electrostatic PEEM [21]. The principle of other electrostatic PEEMs is similar, so the main points can be explained using

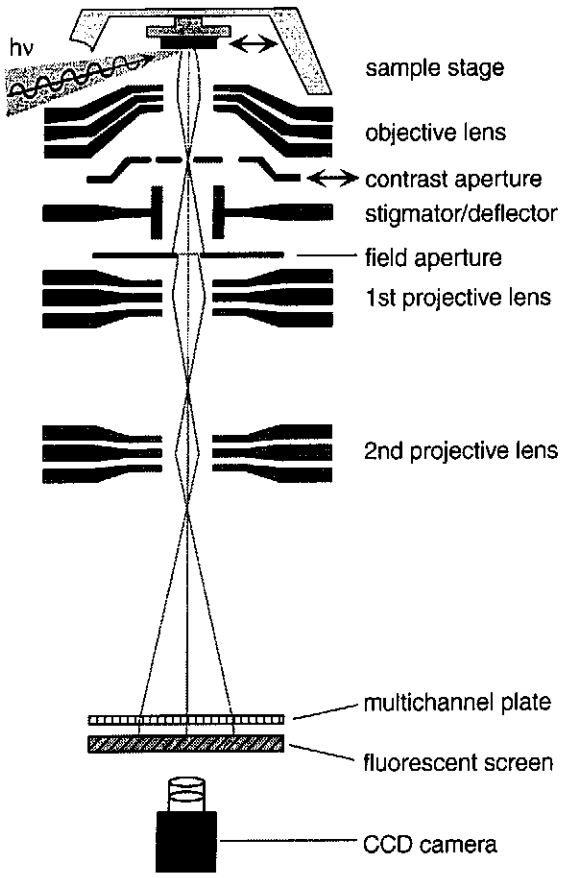

Fig. 1.5. Schematic set up of a photoelectron emission microscope (PEEM). Electrostatic electron lenses create an image of the electrons emitted at the sample surface at a fluorescent screen. (Reproduced from [21] with permission, Copyright (1998) by the World Scientific Publishing Company)

this type. In Fig. 1.5, the sample is shown at the top. It is illuminated by synchrotron radiation under a grazing angle to the sample surface, which is 30 °C in the present example. The sample is kept on ground potential, and electrons are accelerated toward the objective lens, an electrostatic tetrode lens. Typical acceleration voltages are 10–20 kV. The contrast aperture is located in the back focal plane of the objective lens. It selects only those electrons for imaging that originate from a certain range of emission angles. The size and lateral position of this aperture can be changed by moving a slider assembly carrying several apertures of different diameters. In an alternative design, the contrast aperture is located at the back focal plane of the first projective lens [23]. Astigmatism and small misalignments of the optical axis, caused, for example, by a misalignment of the sample, can be corrected by an electrostatic octupole stigmator and deflector. A variable field aperture in the image plane of the objective lens allows one to limit the field of view and to suppress stray electrons. Two electrostatic projective lenses transfer the image onto an imaging unit – which in our example consists of an electron multichannel multiplier and a fluorescent screen on the vacuum side – and charge coupled device (CCD) camera with a conventional lens optics outside the vacuum chamber. Alternative approaches use a glass fiber coupling between the screen and CCD camera [23].

Resolutions down to 20 nm in PEEM imaging using topographic or elemental contrast in threshold photoemission [56] and for excitation with synchrotron radiation [23, 57] have been reported. Even better resolution can be achieved in the LEEM mode, using magnetic objective lenses [25, 26, 58]. Presently, attempts are underway to push the resolution to below 5 nm by aberration correction [59]. In XMCD-PEEM magnetic microspectroscopy, however, intensity is a critical issue. To achieve reasonable acquisition times for the measurement of a complete microscopic and spectroscopic data set, lateral resolution will typically be selected to be a few hundred nanometers in practical microspectroscopy applications.

1.3 About Doing XMCD-PEEM Microspectroscopy

When employing magnetic dichroism effects for the spectroscopy of magnetic materials, the magnetic information is obtained from changes in the spectra that occur either upon changing the magnetization state of the sample or the polarization properties of the exciting radiation. This usually involves the measurement of relatively small differences between large signals and imposes high experimental requirements with respect to signal reproducibility, stability, and flux normalization. The additional imaging step in microspectroscopy is certainly not facilitating the fulfillment of these requirements. In the following, some of the crucial obstacles and their solutions specific to XMCD-PEEM microspectroscopy will be discussed.

1.3.1 Experiment

Let us first consider effects related to the incident radiation. The normalization to the flux of the incoming beam is not straightforward in microspectroscopy, in

contrast to conventional absorption spectroscopy. In the latter, usually the photo yield from a suitable optical element in the beamline or from a specially designed flux monitor is recorded simultaneously to the sample signal. Since the entire photon beam is contributing to both the monitor signal and the signal from the sample, normalization is achieved by simply dividing one by the other. In imaging microspectroscopy, however, the *local* photon flux density is important, not the *integral* flux. It cannot be directly measured and may locally deviate significantly from the integral monitor flux signal. The cause of such deviations may be the radiation characteristics of the insertion devices used in third-generation synchrotron light sources and beamline X-ray optics. An inhomogeneous distribution of the photon intensity within the imaged area on the sample invalidates the normalization to a conventional beam monitor. The fact that the intensity distribution of undulators depends also on the relative photon energy with respect to the maximum of the undulator harmonics complicates matters further. Although in principle these effects cannot be avoided, it is possible from the experimental side to reduce the discrepancy between the local flux density and the integral flux measured by the monitor as much as possible, as described in the following. If the remaining error is below a few percent, it can be approximately corrected out in the course of data analysis, as will be explained in more detail in Sect. 1.3.2.

To get a better correlation between the local and integral photon flux it is important that the illuminated area on the sample be not much bigger than what is imaged in microspectroscopy. All the flux outside the field of view adds an irrelevant contribution to the monitor signal. Attention should also be paid to the adjustment of the imaged area to the center of the undulator radiation. Finally, a significant reduction in photon energy-dependent effects can be achieved when the movement of the insertion device gap can be synchronized with the scanning of the grating of the monochromator.

Local energy resolution is an important issue for those beamline optics where the light spot is an image of the exit slit. In such beamlines, the monochromator energy dispersion at the position of the exit slit is imaged onto the sample surface. As a consequence, the local resolution does not change when the slit size is varied. The more serious implication for microspectroscopy is that there is also photon energy dispersion across the image in this case. If the energy dispersion across the image is of comparable size compared to the width of the spectral features of the sample, this shift in energy across the image has to be considered in data analysis of the microspectra.

A point that is normally not given closer attention in microscopy, but which becomes essential in quantitative microspectroscopy, is the linearity of the image detection system. A typical detection system may consist of several components, for example, a multichannel electron multiplier, fluorescence screen, and CCD camera. Although it is desirable to reach intensities as high as possible to get short exposure and scan times, it may sometimes be necessary to sacrifice some output signal in order to operate in the linear range of the image detection system. This range can be determined beforehand by manipulating the incident beam flux in a controlled way and comparing image intensity and flux monitor signal.